Second harmonic generation on self-assembled GaAs / Au nanowires with thickness gradient

A. Belardini[1,*], G. Leahu[1], M. Centini[1], R. Li Voti[1], E. Fazio[1], C. Sibilia[1], D. Repetto[2], F. Buatier de Mongeot[2]

1. *Dipartimento di Scienze di Base e Applicate per l'Ingegneria, Sapienza Università di Roma, Via A. Scarpa 14, I-00161 Roma, ITALY.*
2. *Dipartimento di Fisica, Università di Genova, Via Dodecaneso 33, I-16146, Genova, ITALY.*

* *email: alessandro.belardini@uniroma1.it*

ABSTRACT

Here we investigated the SH generation at the wavelength of 400 nm (pump laser at 800 nm, 120 fs pulses) of a "metasurface" composed by an alternation of GaAs nano-grooves and Au nanowires capping portions of flat GaAs. The nano-grooves depth and the Au nanowires thickness gradually vary across the sample. The samples are obtained by ion bombardment at glancing angle on a 150 nm Au mask evaporated on a GaAs plane wafer. The irradiation process erodes anisotropically the surface, creating Au nanowires and, at high ion dose, grooves in the underlying GaAs substrate (pattern transfer).

The SHG measurements are performed for different pump linear polarization angle at different positions on the "metasurface" in order to explore the regions with optimal conditions for SHG efficiency. The pump polarization angle is scanned by rotating a half-wave retarder plate. While the output SH signal in reflection is analyzed by setting the polarizer in 's' or 'p' configuration in front of the detector.

The best polarization condition for SHG is obtained in the configuration where the pump and second harmonic fields are both 'p' polarized, and the experiments show a SH polarization dependence of the same symmetry of bulk GaAs. Thus, the presence of gold contributes only as field localization effect, but do not contributes directly as SH generator.

Keywords: GaAs nanostructures, Plasmonics, second harmonic generation from nanostructures, generalized Snell's law.

Nonlinear Optics and Applications X, edited by Mario Bertolotti, Joseph W. Haus, Alexei M. Zheltikov, Proc. of SPIE Vol. 10228, 102280L · © 2017 SPIE · CCC code: 0277-786X/17/$18 · doi: 10.1117/12.2268698

INTRODUCTION

Gallium arsenide (GaAs) nanostructures have attracted a lot of interest for the realization of optical devices such as emitting diodes, nano lasers, nano-element for integrated solar cells, resonant absorbers [nostro sci rep, nostro aom]. Among different possible applications, as others materials with the same wurtzite symmetry, GaAs nanoelements can be used as second harmonic generation (SHG) emitters. Efficient coupling of GaAs emitters with plasmonic gold antennas has been recently investigated [1]. A proper coupling with metal plasmonics modes can enhance the local electro-magnetic field in the GaAs nanoelement, thus increasing the SHG efficiency [2,3].
On the other side, SHG depending on the coupling between electromagnetic radiation and nanostructures modes can be used as a powerful tool in order to characterize the efficiency of the coupling in complex metasurfaces [4,5].
Here we fabricated a "metasurface" composed by self-assembled GaAs nano-grooves capped with gold nanowires which thickness vary along the samples length. By tuning, in this way, the effective plasmonic resonance on gold, results to be tuned also the electromagnetic filed localization in the GaAs groove section, thus producing a SHG signal that can reveal the best coupling conditions.

1. SAMPLE PREPARATION

The sample is obtained by evaporating 150 nm of gold on 0.3 mm GaAs plane wafer, then by fluxing argon ions at a glancing angle (82°) in order to pattern grooves on the sample with increasing thicknesses (see fig.1).

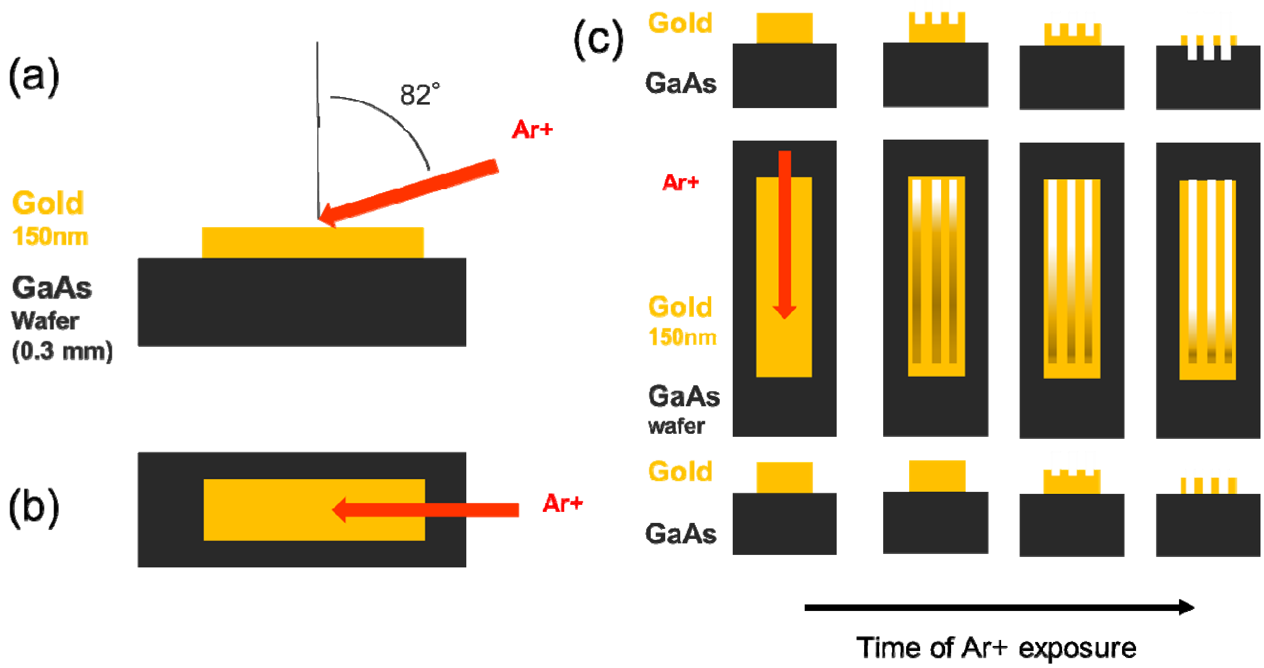

Figure 1: Sample fabrication schemes. (a) Side view of argon flux. (b) top view. (c) Top view of the sample during argon flux as a function of argon time exposure. The lateral views are sketched at the top and bottom of the figures.

The argon flux produces grooves on the flat gold layer (the surface size of the gold layer is 10 mm x 25 mm) that grow as a function of time [6,7]. The grooves are more pronounced close to the top edge of the sample (close to the argon flux origin) and less pronounced close to the bottom edge. With increasing time, under argon fluxing, the grooves on gold arrive at the GaAs substrate level, producing in this way unconnected gold wires. By continuing to flux argon ions the grooves go deeper in GaAs layer (see figure 2).

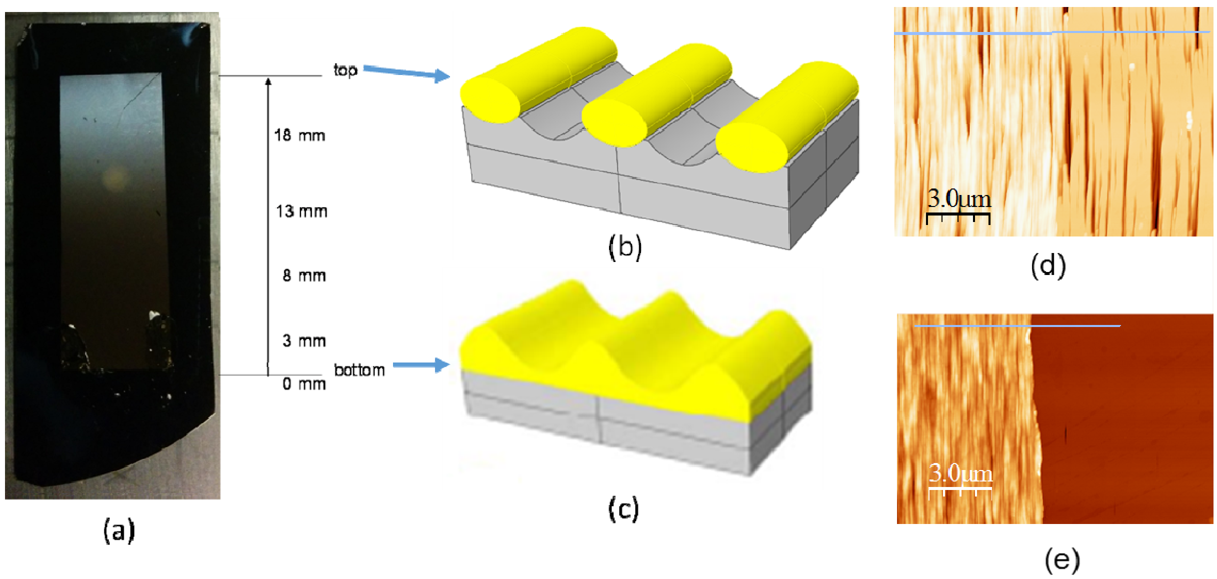

Figure 2: Sample realized with 42 min exposure time. (a) top view image of the sample. (b) 3D sketch of the top part of the sample with gold unconnected nanowires and grooves on GaAs layer. (c) 3D sketch of the bottom part of the sample with grooves on the gold layer that is still connected and untouched GaAs layer. (d) AFM image of the top of the sample, on the right side the AFM in a zone where the gold was removed; (e) AFM image of the bottom of the sample, on the right side the AFM in a zone where the gold was removed

In order to evaluate the proper argon fluxing time the transversal resistance across the gold layer was monitored during grooves formation (see figure 3).

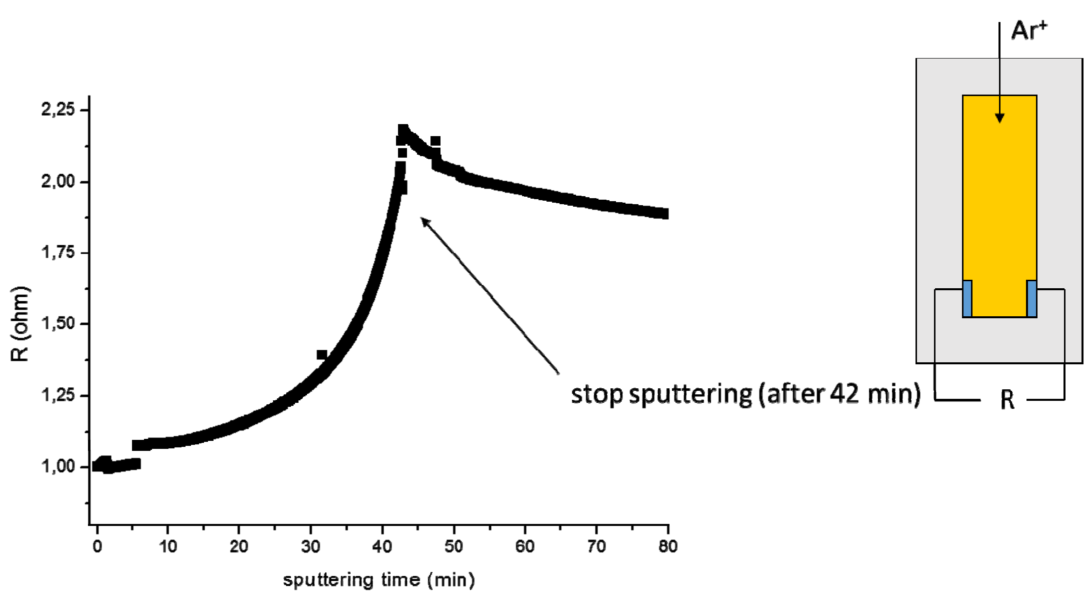

Figure 3: measurement of the transversal resistance during argon flux.

From AFM measurements the formed grooves have an average lateral distance of about 100nm (figure 2d-e). The bottom part of the sample present a gold layer of 80 nm (starting from the original 150 nm flat layer) with grooves of about 30-40 nm. The top part has 40 nm of patterned gold thickness with grooves of about 80nm that penetrate into the GaAs layer.

2. SHG EXPERIMENTS

The SHG measurements are performed in reflection mode at 45° of incidence for different pump linear polarization states and in different positions of the metasurface in order to explore the regions with best condition for SHG efficiency (see figure 4).

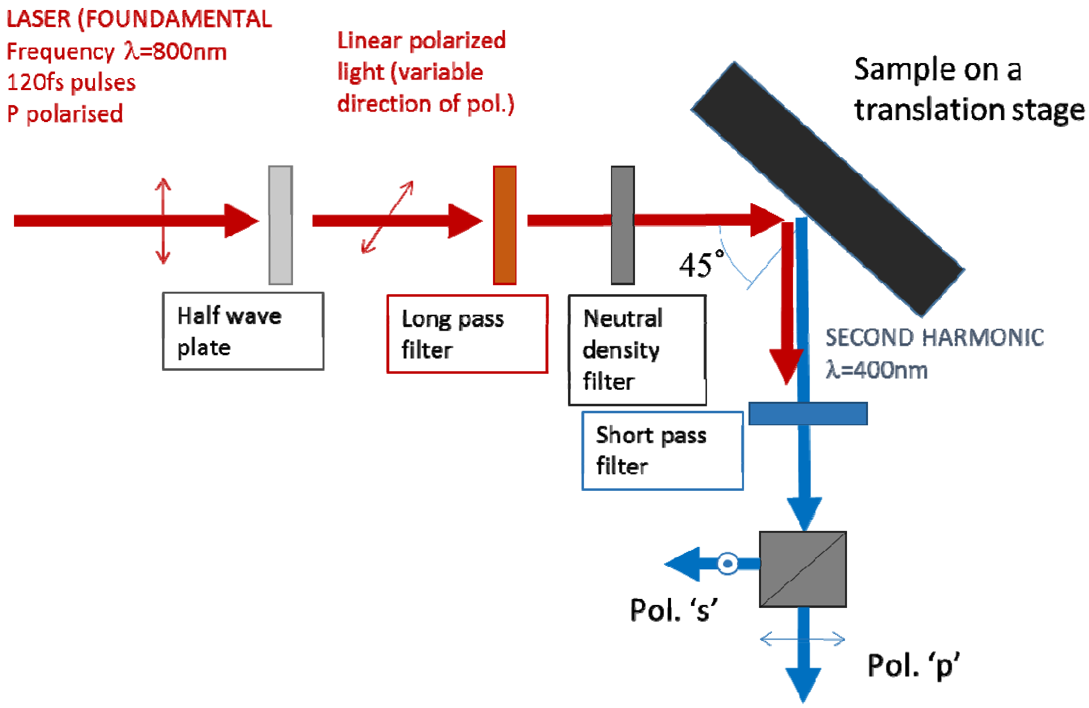

Figure 4: scheme of the SHG experimental setup.

The laser is a P polarised amplified femtosecond Ti:sapphire system with repetition rate of 1kHz, pulse duration 120 fs, central wavelength 800nm, average power on the sample 70mW with a spot size of 1mm in diameter. The pump polarization angle is scanned by rotating a half-wave retarder plate. In our configuration when the waveplate fast axis orientation is at 0° (indicated ad 0° in the measurements graphs) the laser pump results to be P polarized, with the waveplate at 45° the pump results to be S polarized. The output SH signal is analyzed by set the a polarizer in 'S' or 'P' configuration in front of the detector. The SH signal collected in reflection is isolated from the reflected pump at 800 nm by using a series of short pass filters and band pass filters centered around 400 nm.

As a reference, in figure 5, we show the SHG measurements obtained as a function of the half wave plate orientation on a part of the sample where is present the bare flat GaAs substrate (corresponding to -1.5 mm with respect bottom edge of gold zone).

It is worth to note that best SH signal is obtained in P-pump P-second harmonic configuration (P-P), while the P-pump S-second harmonic is forbidden for symmetry reason. The P-second harmonic signal has a one-fold symmetry in the 0°-180° polarization state of the pump (corresponding to 0°-90° in the waveplate fast axis orientation angle), while S-second harmonic signal has a two-fold symmetry.

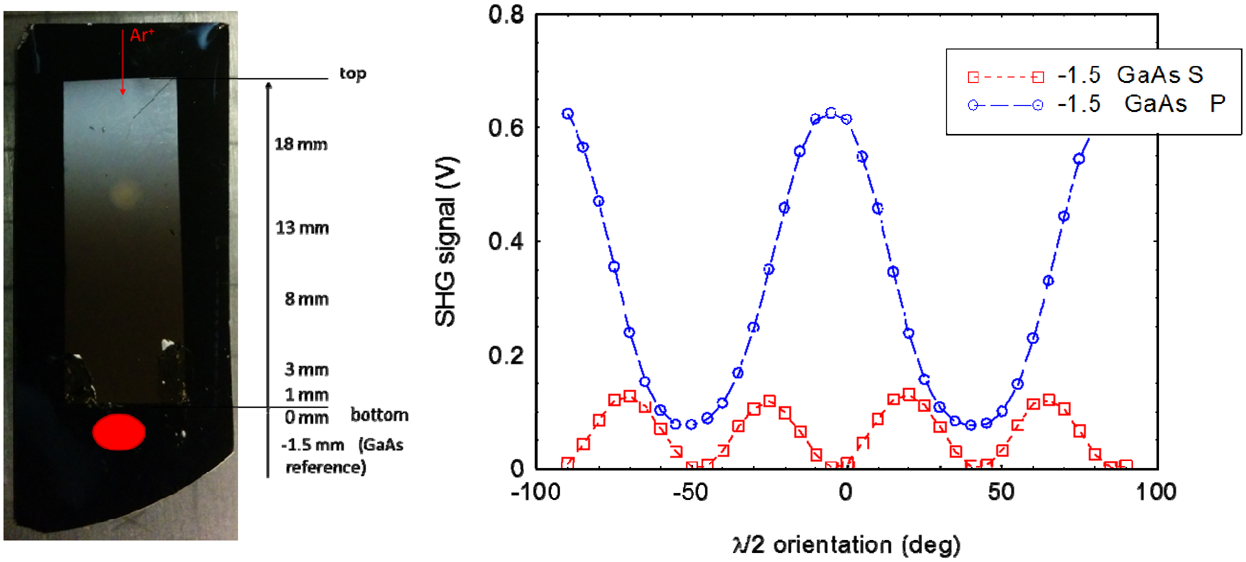

(a) (b)

Figure 5: SHG measurements at -1.5 mm. (a) Top view of the sample where is marked with a red spot the area of the actual SHG measurements. (b) SHG measurements results for S polarized output (red squares) and P polarized output (blue circles).

In figure 6 we show the SHG measurements results in a region of patterned gold close to the bottom edge (at 1 mm to the bottom edge).

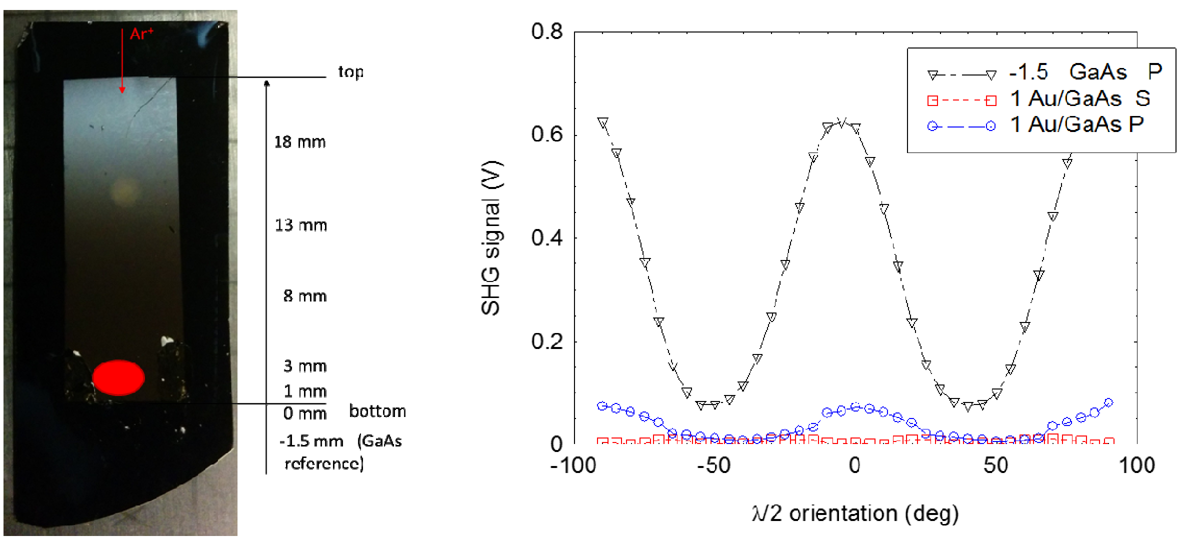

(a) (b)

Figure 6: SHG measurements at 1 mm. (a) Top view of the sample where is marked with a red spot the area of the actual SHG measurements. (b) SHG measurements results for S polarized output (red squares) and P polarized output (blue circles). In black triangles are reported the reference measurements obtained on GaAs (-1.5 mm) for the best configuration (P-P).

It that part of the sample is present a connected gold layer of about 80 nm with grooves on it wich thickness is about 20 – 30 nm. The SHG signal due to the gold layer is about 10 times less with respect the GaAs flat surface, but with similar SH polarization symmetry.

In figure 7 we report the SHG measurements obtained at 3 mm from the bottom edge. Here the gold layer is almost still connected, but the grooves are more pronounced.

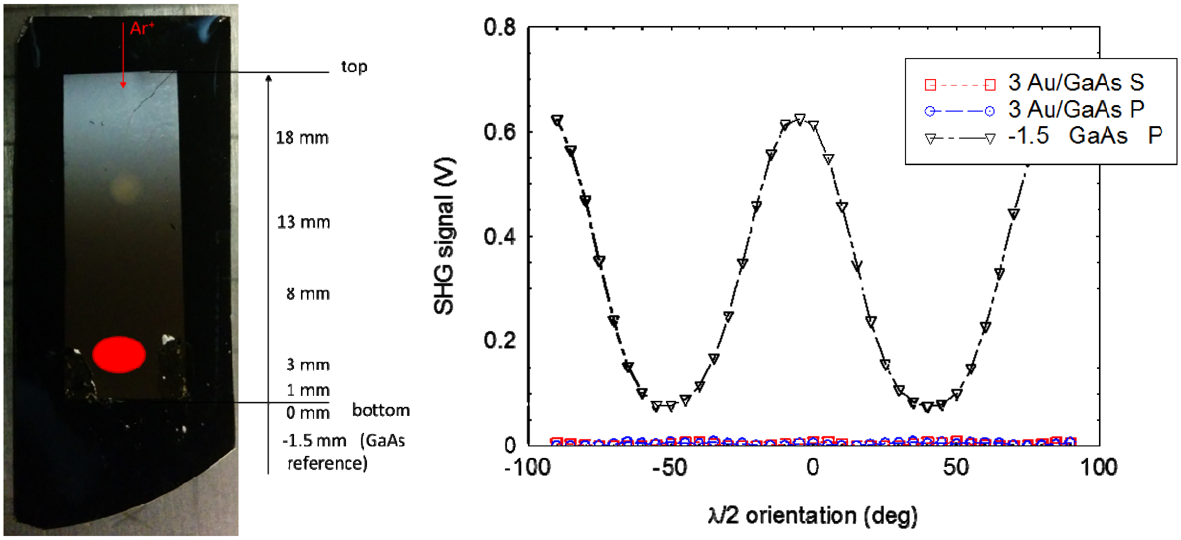

(a) (b)

Figure 7: SHG measurements at 3 mm. (a) Top view of the sample where is marked with a red spot the area of the actual SHG measurements. (b) SHG measurements results for S polarized output (red squares) and P polarized output (blue circles). In black triangles are reported the reference measurements obtained on GaAs (-1.5 mm) for the best configuration (P-P).

The SHG is very low even with respect to gold, thus indicating dominant losses due to scattering form grooves.

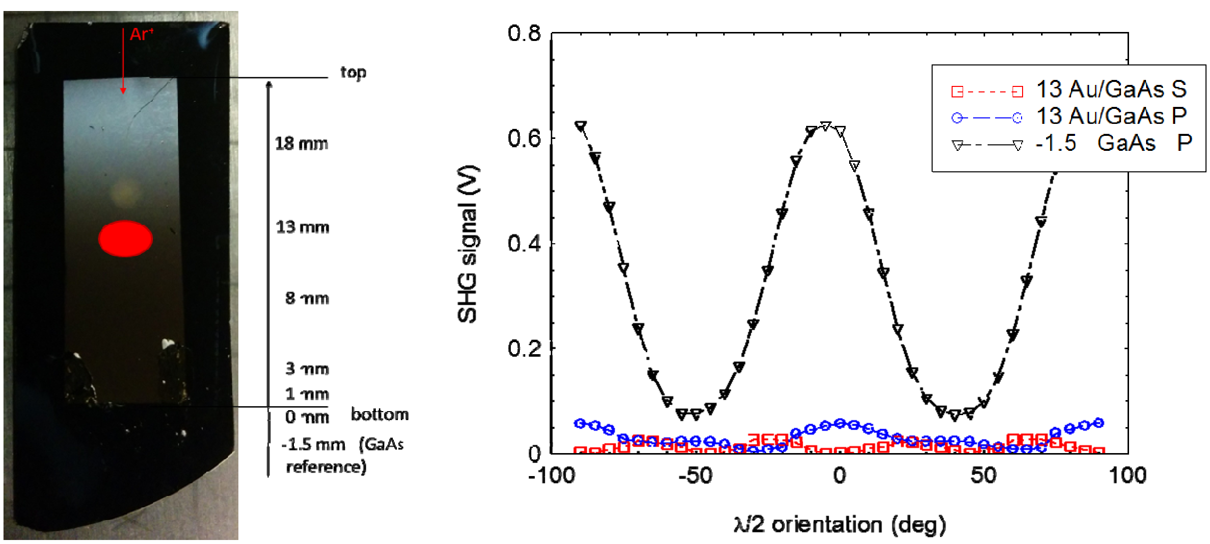

(a) (b)

Figure 8: SHG measurements at 13 mm. (a) Top view of the sample where is marked with a red spot the area of the actual SHG measurements. (b) SHG measurements results for S polarized output (red squares) and P polarized output (blue circles). In black triangles are reported the reference measurements obtained on GaAs (-1.5 mm) for the best configuration (P-P).

By going close to the centre of the sample (13mm), we consider a region where gold layer is disconnected forming wires on grooves in GaAs. Light can excite the higher second order nonlinear coefficient of GaAs with respect to gold, indeed in figure 8 SHG efficiency increase again even if the losses induced by scattering can be higher due to the deepest grooves. A notable feature is the presence in the SHG signal of a two-fold symmetry for P-second harmonic field that is not present in bare GaAs or Au substrates. This is a clear sign of a different localization of the electromagnetic field in the GaAs grooves due to the interaction with plasmonic resonances of the gold capping wires.

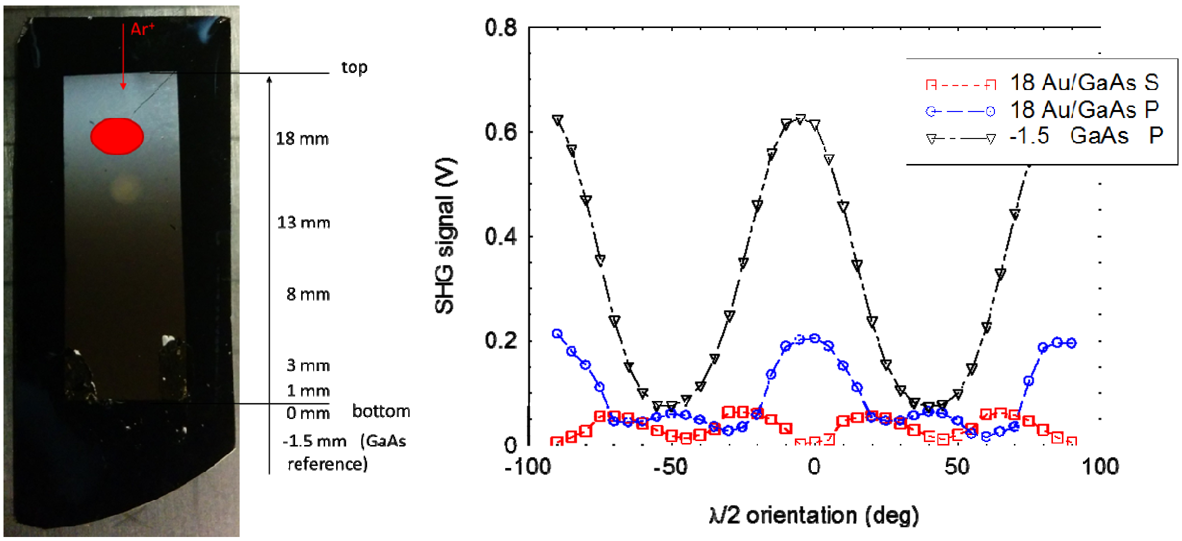

(a) (b)

Figure 9: SHG measurements at 18 mm. (a) Top view of the sample where is marked with a red spot the area of the actual SHG measurements. (b) SHG measurements results for S polarized output (red squares) and P polarized output (blue circles). In black triangles are reported the reference measurements obtained on GaAs (-1.5 mm) for the best configuration (P-P).

In figure 9 are reported the SHG measurements in a region close to top part (18 mm from the bottom). In this region the grooves go deeper in the GaAs layer with an average penetration of 40nm. The gold wires thickness is about 30-40 nm. The measurements show an increment of the SHG signal due to a better Au-GaAs interaction.

3. DEVIATION MEASUREMENTS

Even if the SHG signal did not get the conversion efficiency of the pure GaAs substrate, it is evident the effect the a gradual increasing of the electromagnetic field interaction with metasurface. This will produce a gradient in the phase shift felt be the light when is reflected by the metasurface as predicted by the modified Snell's law of refraction and reflection, described by Capasso and co-workers in [8], for the case of the transmission of light passing from a medium 1 to a medium 2:

$$n_2 \cdot \sin(\theta_2) - n_1 \cdot \sin(\theta_1) = \frac{\lambda_0}{2\pi} \cdot \frac{d\Phi(x)}{dx} \quad , \qquad (1)$$

where n_1 and n_2 are the refractive indices of the media 1 and 2 respectively, λ_0 is the beam wavelength and $\Phi(x)$ represents the phase discontinuity introduced by the nanostructure at the point x of the interface, θ_2 is the refracted angle, θ_1 is the incidence angle.
In the case of reflection eq.1 becomes:

$$\sin(\theta_2) - \sin(\theta_1) = \frac{\lambda_0}{2\pi \cdot n_1} \cdot \frac{d\Phi(x)}{dx} \quad , \qquad (2)$$

where is present the only n_1 index of refraction of the incident medium, θ_2 is the reflected acted angle, θ_1 is the incidence angle.

In our works [9-11] we demonstrated that is possible to use a simple deviation measurement setup in order to measure the anomalous reflection and, thus, to verify the gradient induced by plamonic metasurfaces. In this work we realized the setup described in fig.10.

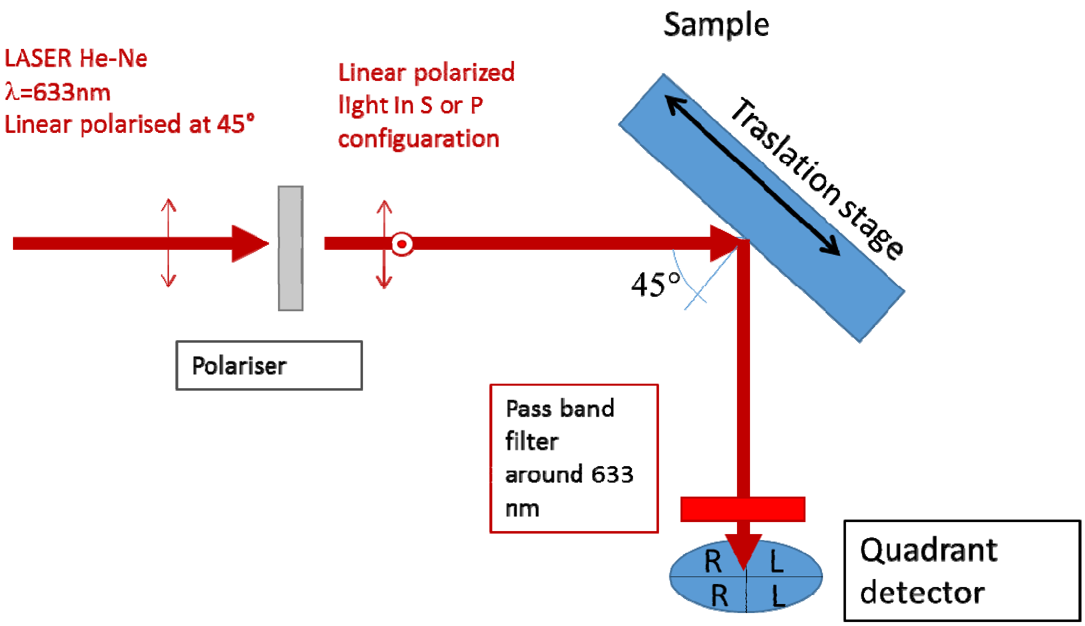

Figure 10: Deviation measurement setup.

The light source is a He-Ne laser emitting at 633nm with a collimated spot size of less than 1 mm in diameter. The polarization of the light can be set to S or P polarization state. The light is then sent onto the meatsurface sample at an incidence angle of 45°. The spot of incidence can be scanned by motorized translation stage connected to a computer. The reflected light is detected by a 8 mm diameter photodiode divided in sectors (labeled *L* for left side sectors and *R* for right side sectors in Fig.10). The detector is posed at a distance *D=400 mm* far away from the sample surface. The output of the sensor was analysed by a position detector circuit giving at the same time the total power

$$P_T = P_L + P_R \quad , \tag{3}$$

impinging on the detector and the normalised difference between the power of the light in the sectors *L* and the power of the light in sectors *R*:

$$X = \frac{P_L - P_R}{P_T} \quad . \tag{4}$$

The P_T value is supplied in volts at the output of the circuit and is proportional to the total power by a conversion factor of 0.5 mW/V. The *X* value is proportional to the displacement of the beam with respect to the centre of the detector and was supplied in volts at the output of the circuit. Measurements conversion from the circuit signal (in volts) to the real displacement (in mm) is retrieved by a calibration measurement and results to be 0.05mm/V [11,12]. Thus it is possible to retrieve the anomalous reflected angle, $\sin(\theta) = \sin(\theta_2) - \sin(\theta_1) = \frac{\lambda_0}{2\pi \cdot n_1} \cdot \frac{d\Phi(x)}{dx}$ as :

$$\theta \cong \sin(\theta) \cong \mathrm{atan}\left(\frac{X\,[mm]}{D\,[400mm]}\right) \cong \frac{X}{D} \quad . \tag{5}$$

In our sample the deviation induced by the simple geometrical optical propagation is polarization insensitive (i.e. wedge effect), while the phase shift accumulates by the electromagnetic field due to the metasurface interaction depends on the coupling between plasmonic gold modes and nano-structured GaAs modes and thus is polarization dependent. For this reason, in figure 11 we show the difference of the deviation induced by P polarized light and S polarized light.

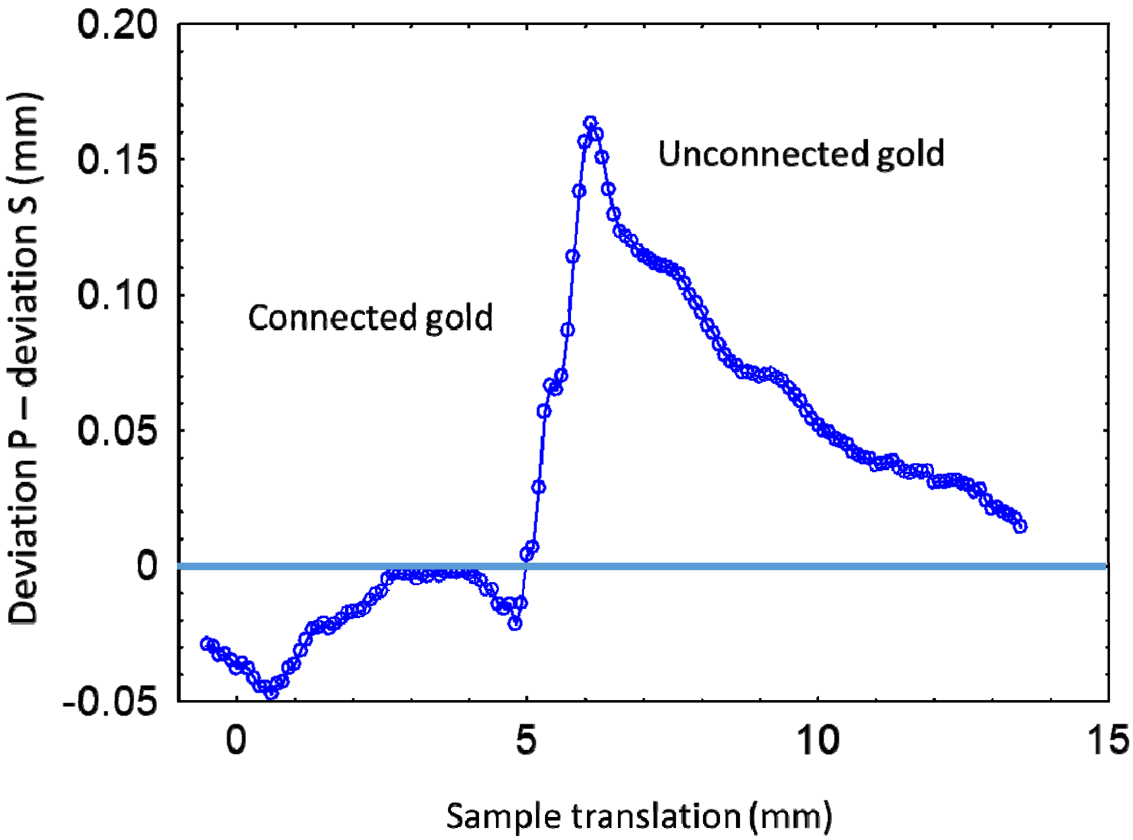

Figure 11: Difference between the deviation obtained in P polarization with the deviation obtained in S polarization.

In the measurements shown in figure 11 it evident that as the light impinges on connected gold (even if the gold is patterned), there are no great difference between polarizations, thus indicates that the deviation is due mostly on geometrical features. While the gold become disconnected and GaAs patterned substrate become accessible the anomalous reflection induced by GaAs-gold interaction is evident, confirming the results obtained by SHG measurements.

4. CONCLUSIONS

We experimentally investigated the second harmonic signal generated by a "metasurface" composed by self-assembled GaAs nano-grooves capped with gold nanowires which thickness vary along the samples length. The tuning of the effective coupling between the plasmonic resonance on gold and nano-patterned GaAs layer induced an electromagnetic filed localization in the GaAs groove section, thus producing a SHG signal that increases as the grooves become deeper.

The electromagnetic (e.m.) field localization is evidenced also by anomalous reflection measurements that are sensitive to e.m. phase accumulation.
The obtained results worth to be further investigated by measuring samples with deeper grooves that we are presently realizing.

REFERENCES

[1] A. Casadei, E. F. Pecora, J. Trevino, C. Forestiere, D. Rüffer, E. Russo-Averchi, F. M.atteini, G. Tutuncuoglu, M. Heiss, A. Fontcuberta i Morral, and L. Dal Negro, "Photonic–Plasmonic Coupling of GaAs Single Nanowires to Optical Nanoantennas," Nano Lett. 14, 2271–2278 (2014).

[2] T. Skauli, K. L. Vodopyanov, T. J. Pinguet, A. Schober, O. Levi, L. A. Eyres, M. M. Fejer, J. S. Harris, B. Gerard, L. Becouarn, E. Lallier, and G. Arisholm, "Measurement of the nonlinear coefficient of orientation-patterned GaAs and demonstration of highly efficient second-harmonic generation," Opt. Lett. 27, 628 (2002).

[3] A. M. Malvezzi, G. Vecchi, M. Patrini, G. Guizzetti, L. C. Andreani, F. Romanato, L. Businaro, E. Di Fabrizio, A. Passaseo, and M. De Vittorio, "Resonant second-harmonic generation in a GaAs photonic crystal waveguide," Phys. Rev. B 68, 161306(R) (2003).

[4] A. Belardini, Benedetti, A., Centini, M., Leahu, G., Mura, F., Sennato, S., Sibilia, C., Robbiano, V., Giordano, M. C., Martella, C., Comoretto, D. and de Mongeot, F. B. Advanced Optical Materials 2, 208–213 (2014).

[5] A. Belardini, M. Centini, G. Leahu, D. C. Hooper, R. Li Voti, E. Fazio, J. W. Haus, A. Sarangan, V. K. Valev, C. Sibilia, Sci. Rep. 6, 31796 (2016).

[6] D. Chiappe, Toma, A., De Mongeot, F.B. Small 9, 913-919 (2013).

[7] G. Della Valle, Polli, D., Biagioni, P., Martella, C., Giordano, M.C., Finazzi, M., Longhi, S., Duò, L., Cerullo, G., Buatier De Mongeot, F. Physical Review B 91, 235440 (2015).

[8] N. Yu, Genevet, P., Kats, M. A., Aieta, F., Tetienne, J.-P., Capasso, F., Gaburro, Z., "Light Propagation with Phase Discontinuities: Generalized Laws of Reflection and Refraction," Science 334, 333-337 (2011).

[9] A. Belardini, Pannone, F., Leahu, G., Larciprete, M. C., Centini, M., Sibilia, C., Martella, C., Giordano, M., Chiappe, D., and Buatier de Mongeot, F., "Evidence of anomalous refraction of self-assembled curved gold nanowires," Appl. Phys. Lett. 100, 251109 (2012).

[10] A. Belardini, Pannone, F., Leahu, G., Larciprete, M. C., Centini, M., Sibilia, C., Martella, C., Giordano, M., Chiappe, D., and Buatier de Mongeot, F., "Asymmetric transmission and anomalous refraction in metal nanowires metasurface," J. Europ. Opt. Soc. Rap. Public. 7, 12051 (2012).

[11] A. Belardini, G. Leahu, M. C. Larciprete, M. Centini, C. Sibilia, C. Martella, M. Giordano, D. Chiappe, F. Buatier de Mongeot, "Anomalous refraction of self assembled gold nanowires studied by the generalized Snell's law," Photonics Lett. of Poland 5, 45-47 (2013).

[12] A. Belardini, C. Sibilia, "Evaluation of the negative refractive index by beam deviation measurements," Optoelectron. Adv. Mater.–Rapid Commun. 7, 184 (2013).